

Electronic Supplementary Information (ESI) for

Highly selective and controllable pyrophosphate induced anthracene-excimer formation in water

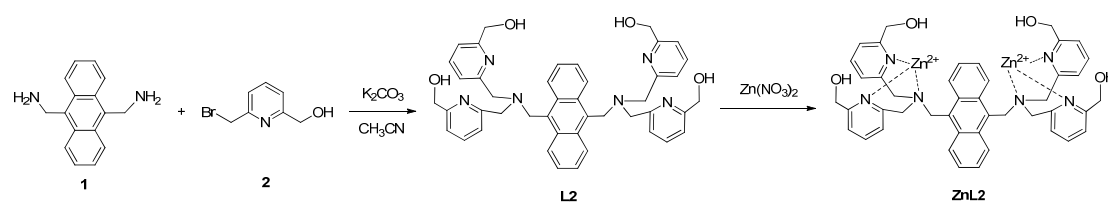
Feihu Huang and Guoqiang Feng*

*Key Laboratory of Pesticide and Chemical Biology of Ministry of Education, College of Chemistry,
Central China Normal University, Wuhan 430079, P.R. China,
gf256@mail.ccnu.edu.cn*

1. General Experimental Details.

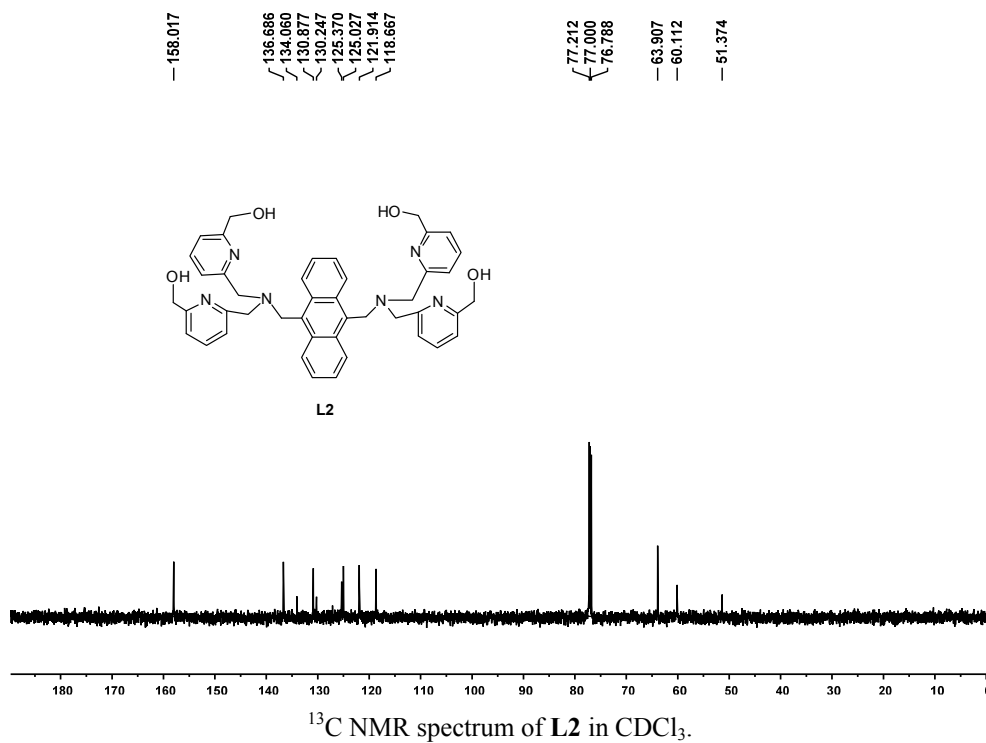
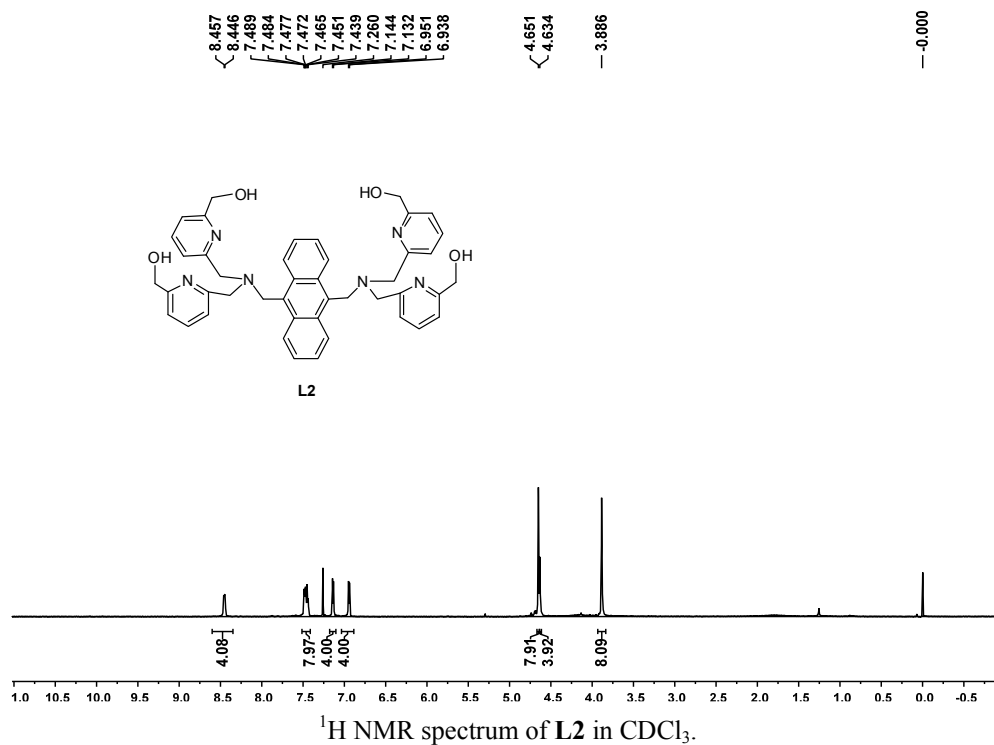
Starting materials were purchased from commercial suppliers and were used without further purification. 9,10-bisaminomethylanthracene¹ and 2-bromomethyl-6-hydroxymethylpyridine² were prepared according the previously published methods. All solvents were purified by the most used methods before use. N-(2-hydroxyethyl)piperazine-N'-(2-ethane-sulfonic acid) (HEPES) was used to prepare buffer solution and all solutions were prepared with using distilled water that had been passed through a Millipore-Q ultrapurification system. NMR spectra were measured on Varian Mercury 400 and 600 instruments. UV-vis spectra and fluorescent spectra were recorded on an Agilent Cary 100 UV-vis spectrophotometer and an Agilent Cary Eclipse fluorescence spectrophotometer, respectively. Both UV-vis and fluorescence spectrophotometer are equipped with a temperature controller. Standard quartz cuvettes with a 10 mm lightpath are used for all UV-vis spectra and fluorescent spectra measurements.

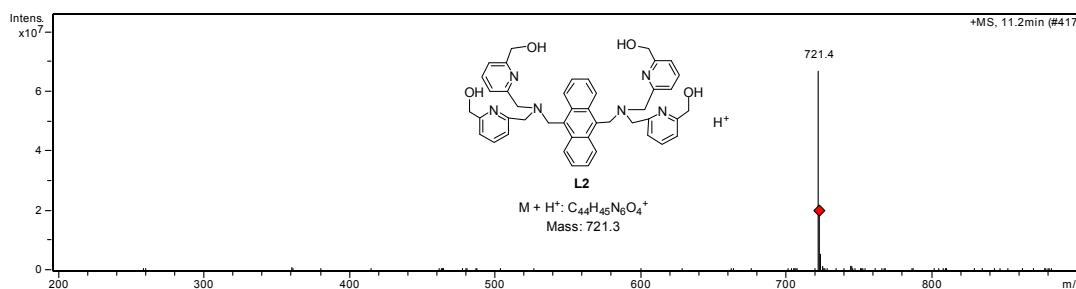
2. Synthesis of ZnL2



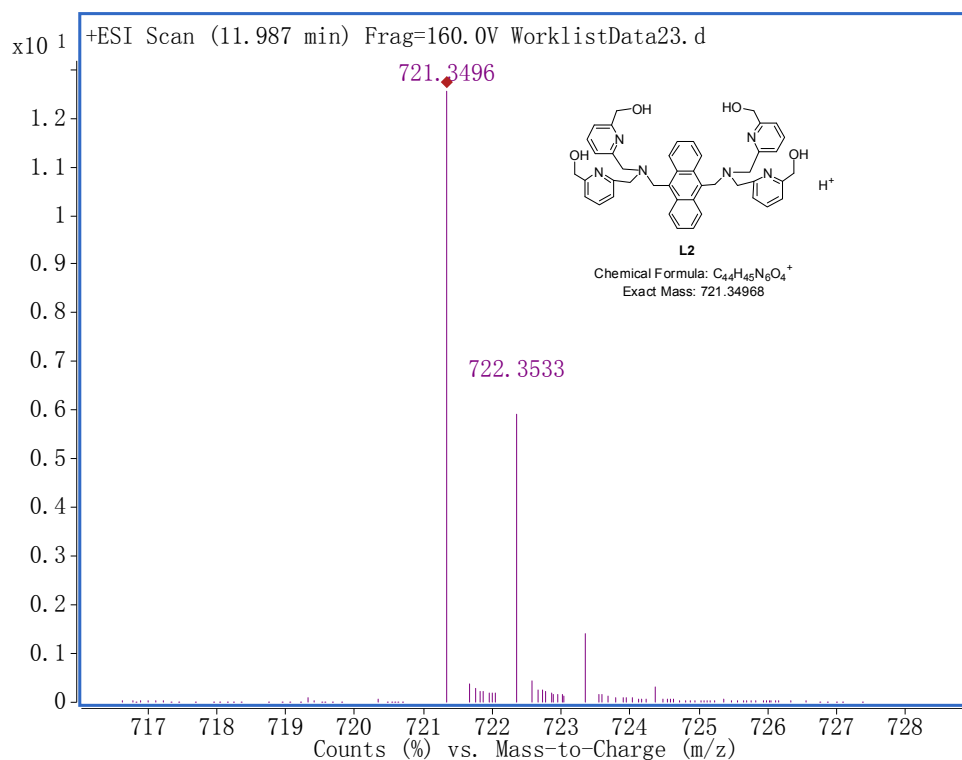
Synthesis of L2: To a solution of **1**¹ (236 mg, 1.00 mmol) and **2**² (810 mg, 4.01 mmol) in anhydrous CH_3CN (30 mL) was added K_2CO_3 (621 mg, 4.50 mmol). The reaction mixture was then heated to reflux for 12 hours, and the solvent was evaporated under reduced pressure. To the residue was added dichloromethane (60 mL), and the organic phase was washed with water and brine followed by drying over $MgSO_4$. After removal of the solvent under reduced pressure, the crude product was purified by silica gel column (eluent: dichloromethane /methanol = 15:1 (v/v)) to give a yellow powder (576 mg, 80% yield). Mp 118–120 °C. 1H NMR (600 MHz, $CDCl_3$) δ 8.45 (d, J = 6.3 Hz, 4H), 7.44–7.49 (m, 8H),

7.13 (d, $J = 7.6$ Hz, 4H), 6.95 (d, $J = 7.6$ Hz, 4H), 4.65 (s, 8H), 4.63 (s, 4H), 3.89 (s, 8H). ^{13}C NMR (150 MHz, CDCl_3): δ 158.0, 136.7, 134.1, 130.9, 130.2, 125.4, 125.0, 121.9, 118.7, 63.9, 60.1, 51.4. IR (KBr) ν_{max} (cm^{-1}): 3393 (br s, OH), 2855, 1595 (s), 1577 (s), 1454 (s), 1354, 1153, 1067, 995, 789, 760, 703; ESI-MS: m/z found 721.4 ($\text{M} + \text{H}^+$); HR-MS Calc. for $\text{C}_{44}\text{H}_{45}\text{N}_6\text{O}_4^+$ ($\text{M} + \text{H}^+$) 721.3497, found 721.3496.





ESI-MS spectrum of **L2**



HR-MS spectrum of **L2**

Synthesis of ZnL2: To a solution of **L2** (36 mg, 0.05 mmol) in 5 mL of MeOH, was added $\text{Zn}(\text{NO}_3)_2 \cdot 6\text{H}_2\text{O}$ (33 mg, 0.11 mmol), and the mixture was stirred for 1 h at rt. After concentrating under reduced pressure, the obtained solid was recrystallised from MeOH to give **ZnL2**. ^1H NMR (400 MHz, D_2O): 8.44(4H, br, PyH), 7.68 (4H, d, $J = 4.8$ Hz, PyH), 7.47 (4H, dd, $J = 4.8$ Hz, PyH), 6.95 (4H, d, ArH), 6.37 (4H, br, ArH), 5.11 (4H, br, 2CH_2), 4.61 (4H, br, 2CH_2), 4.52 (4H, br, 2CH_2), 4.24 (4H, br, 2CH_2), 4.09 (4H, br, 2CH_2). Crystal of **ZnL2** suitable for X-ray diffraction studies was obtained from a solution of **ZnL2** in a mixture of MeOH and water after addition of NaCl. Each complex molecule contains two CH_3OH and two NO_3^- as counter ions. The total formula of **ZnL2** crystal is $\text{C}_{46}\text{H}_{52}\text{Cl}_2\text{N}_8\text{O}_{12}\text{Zn}_2$ ($\text{C}_{44}\text{H}_{44}\text{Cl}_2\text{N}_6\text{O}_4\text{Zn}_2^{2+} \cdot 2\text{CH}_3\text{OH} \cdot 2\text{NO}_3^-$), $M = 1110.62$. [CCDC 949746](#) contains the supplementary crystallographic data for this paper. These data can be obtained free of charge from the Cambridge Crystallographic Data Centre via www.ccdc.cam.ac.uk/data_request/cif.

Crystal data for ZnL2:

Table 1. Crystal data and structure refinement for mo_111219a_0m.

Identification code	mo_111219a_0m	
Empirical formula	C23 H26 Cl N4 O6 Zn	
Formula weight	555.30	
Temperature	100(2) K	
Wavelength	0.71073 Å	
Crystal system	Monoclinic	
Space group	P2(1)/n	
Unit cell dimensions	a = 14.6762(14) Å	$\alpha = 90^\circ$
	b = 8.8145(8) Å	$\beta = 92.436(2)^\circ$
	c = 17.7485(16) Å	$\gamma = 90^\circ$
Volume	2293.9(4) Å ³	
Z	4	
Density (calculated)	1.608 Mg/m ³	
Absorption coefficient	1.237 mm ⁻¹	
F(000)	1148	
Crystal size	0.16 x 0.12 x 0.10 mm ³	
Theta range for data collection	1.76 to 26.00°.	
Index ranges	-18<= <i>h</i> <=18, -10<= <i>k</i> <=10, -19<= <i>l</i> <=21	
Reflections collected	15921	
Independent reflections	4489 [R(int) = 0.0465]	
Completeness to theta = 26.00	99.6 %	
Absorption correction	None	
Max. and min. transmission	0.8863 and 0.8267	
Refinement method	Full-matrix least-squares on F ²	
Data / restraints / parameters	4489 / 10 / 334	
Goodness-of-fit on F ²	1.092	
Final R indices [I>2sigma(I)]	R1 = 0.0402, wR2 = 0.1055	
R indices (all data)	R1 = 0.0591, wR2 = 0.1194	
Extinction coefficient	0.0030(6)	
Largest diff. peak and hole	0.834 and -0.465 e. ⁻³	

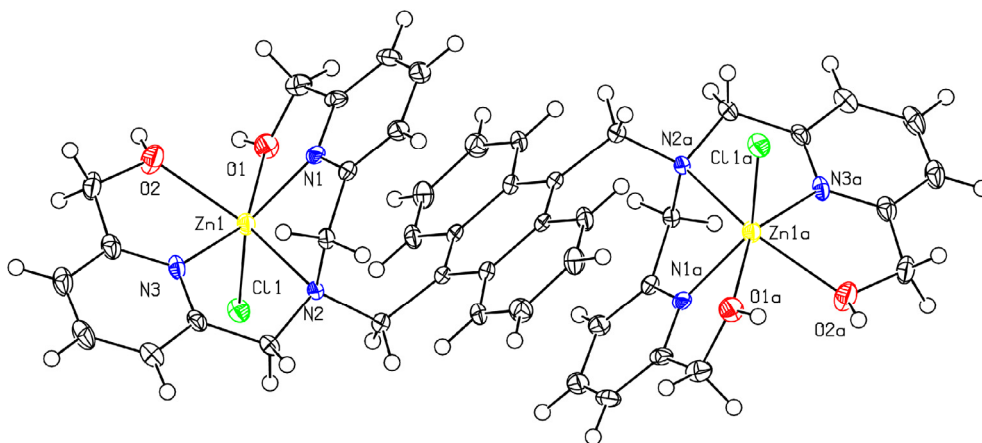
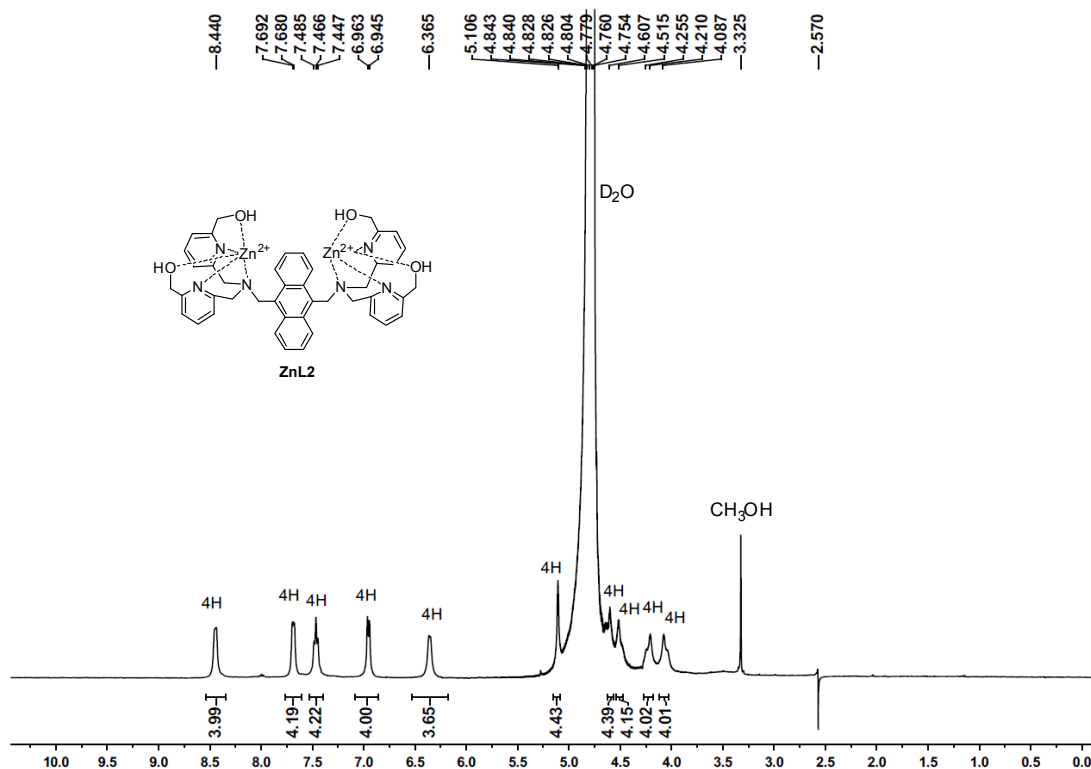


Fig. S1. The crystal structure of **ZnL2**

¹H NMR spectrum of **ZnL2** in D₂O

References:

1. (a) Gassensmith, J. J.; Arunkumar, E.; Barr, L.; Baumes, J. M.; DiVittorio, K. M.; Johnson, J. R.; Noll, B. C.; Smith, B. D. *J. Am. Chem. Soc.* **2007**, *129*, 15054–15059. (b) Gunnlaugsson, T.; Davis, A. P.; O'Brien, J. E.; Glynn, M. *Org. Lett.* **2002**, *4*, 2449–2452. (c) Gunnlaugsson, T.; Davis, A. P.; O'Brien, J. E.; Glynn, M. *Org. Biomol. Chem.* **2005**, *3*, 48–56.
2. Thiabaud, G.; Guillemot, G.; Schmitz-Afonso, I.; Colasson, B.; Reinaud, O. *Angew. Chem., Int. Ed.* **2009**, *48*, 7383–7386.

3. Fluorescence spectra changes of ZnL2 (5 μM) upon addition of different anions

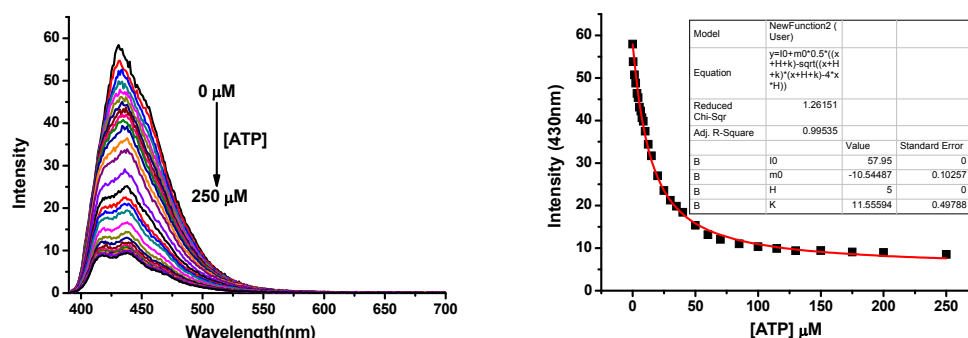


Fig. S2 Left: Fluorescent titration of complex **ZnL2** (5 μM) upon the addition of ATP (0-250 μM) in pH = 7.2, 10 mM HEPES buffer solution at 25°C; Right: The saturation curve of fluorescent intensity changes at 430 nm, λ_{ex} = 380 nm, d_{ex} = 5 nm, d_{em} = 2.5 nm. Red line is the curve fitting using a 1:1 binding mode, and the K_a between **ZnL2** and ATP was determined to be about $8.65 \times 10^4 \text{ M}^{-1}$ ($R^2 = 0.99535$) under this condition.

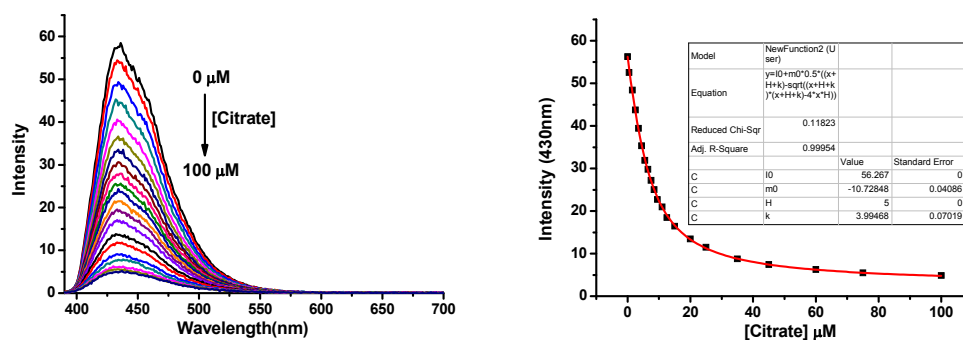


Fig. S3 Left: Fluorescent titration of complex **ZnL2** (5 μM) upon the addition of citrate (0-100 μM) in pH = 7.2, 10 mM HEPES buffer solution at 25°C; Right: The saturation curve of fluorescent intensity changes at 430 nm, λ_{ex} = 380 nm, d_{ex} = 5 nm, d_{em} = 2.5 nm. Red line is the curve fitting using a 1:1 binding mode, and the K_a between **ZnL2** and citrate was determined to be about $2.51 \times 10^5 \text{ M}^{-1}$ ($R^2 = 0.99954$) under this condition.

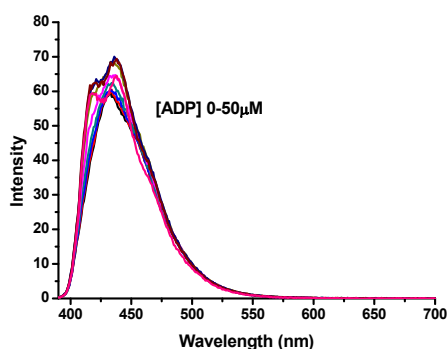


Fig. S4. Fluorescent titration of complex **ZnL2** (5 μM) upon the addition of ADP (0-50 μM) in pH = 7.2, 10 mM HEPES buffer solution at 25°C, λ_{ex} = 380 nm, d_{ex} = 5 nm, d_{em} = 2.5 nm.

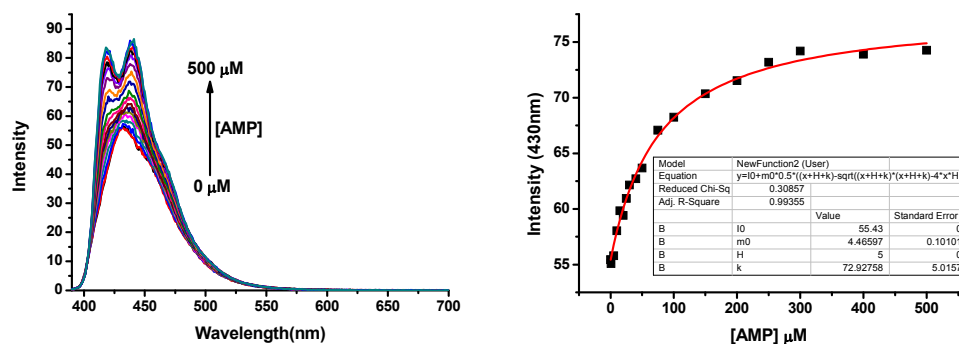


Fig. S5. Left: Fluorescent titration of complex **ZnL2** (5 μM) upon the addition of AMP (0-500 μM) in pH = 7.2, 10 mM HEPES buffer solution at 25°C; Right: The saturation curve of fluorescent intensity changes at 430 nm, λ_{ex} = 380 nm, d_{ex} = 5 nm, d_{em} = 2.5 nm. Red line is the curve fitting using a 1:1 binding mode, and the K_a between **ZnL2** and AMP was determined to be about $1.37 \times 10^4 \text{ M}^{-1}$ ($R^2 = 0.99355$) under this condition.

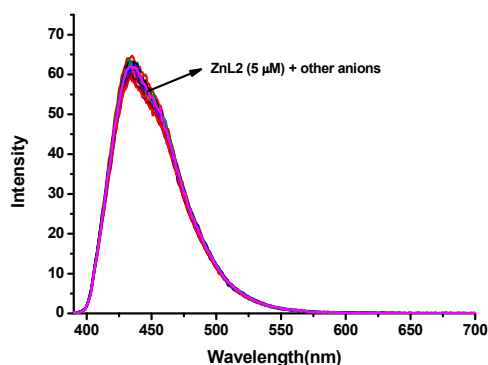


Fig. S6. Fluorescent titration of complex **ZnL2** (5 μM) upon the addition of other anions (PO_4^{3-} , HPO_4^{2-} , H_2PO_4^- , F^- , Cl^- , Br^- , I^- , ClO_4^- , AcO^- , CO_3^{2-} , HCO_3^- , SO_4^{2-} , HSO_4^- , NO_3^- , N_3^- , NO_2^- , SCN^- , $\text{S}_2\text{O}_3^{2-}$, $\text{S}_2\text{O}_7^{2-}$, 50 μM of each was used) in pH = 7.2, 10 mM HEPES buffer solution, λ_{ex} = 380 nm, d_{ex} = 5 nm, d_{em} = 2.5 nm.

4. Fluorescence spectra changes of ZnL2 (50 μM) upon addition of different anions

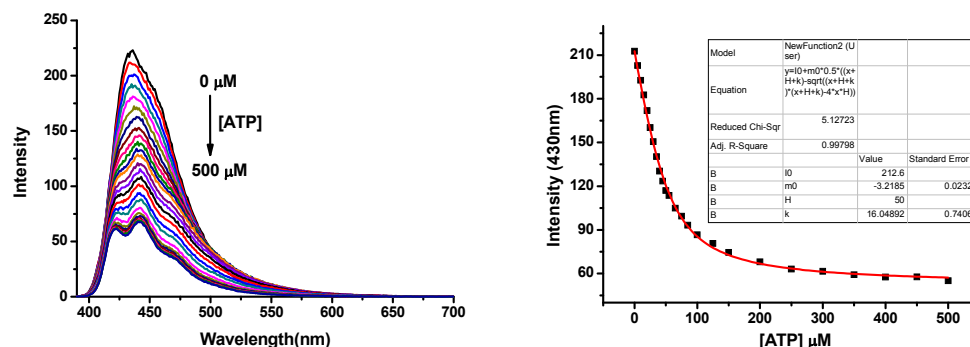


Fig. S7. Left: Fluorescent titration of complex **ZnL2** (50 μM) upon the addition of ATP (0-500 μM) in pH = 7.2, 10 mM HEPES buffer solution at 25°C; Right: The saturation curve of fluorescent intensity changes at 430 nm, $\lambda_{\text{ex}} = 380$ nm, $d_{\text{ex}} = d_{\text{em}} = 2.5$ nm. Nonlinear least-squares fitting the fluorescent titration curve gave K_a between **ZnL2** and ATP is $6.23 \times 10^4 \text{ M}^{-1}$ ($R^2 = 0.99798$) under this condition.

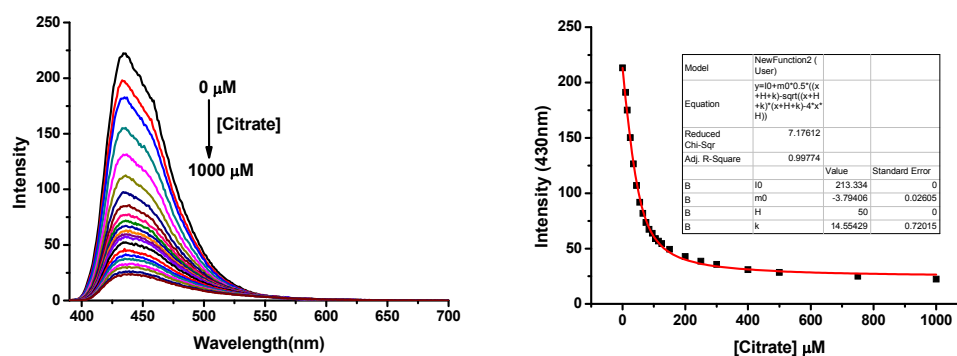


Fig. S8. Left: Fluorescent titration of complex **ZnL2** (50 μM) upon the addition of citrate (0-1000 μM) in pH = 7.2, 10 mM HEPES buffer solution at 25°C; Right: The saturation curve of fluorescent intensity changes at 430 nm, $\lambda_{\text{ex}} = 380$ nm, $d_{\text{ex}} = d_{\text{em}} = 2.5$ nm. Nonlinear least-squares fitting the fluorescent titration curve gave K_a between **ZnL2** and citrate is $6.87 \times 10^4 \text{ M}^{-1}$ ($R^2 = 0.99774$) under this condition.

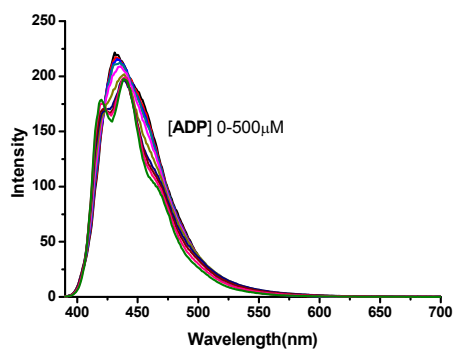


Fig. S9. Fluorescent titration of complex **ZnL2** (50 μM) upon the addition of ADP (0-500 μM) in pH = 7.2, 10 mM HEPES buffer solution at 25°C, $\lambda_{\text{ex}} = 380$ nm, $d_{\text{ex}} = d_{\text{em}} = 2.5$ nm.

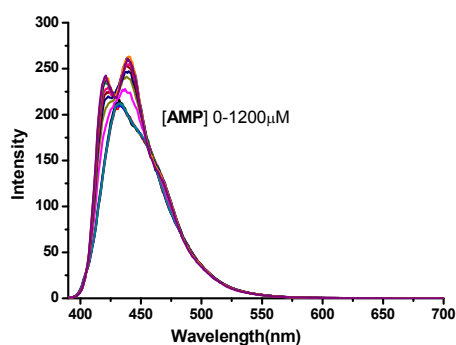


Fig. S10. Fluorescent titration of complex **ZnL2** (50 μM) upon the addition of AMP (0-1200 μM) in pH = 7.2, 10 mM HEPES buffer solution at 25°C, λ_{ex} = 380 nm, d_{ex} = d_{em} = 2.5 nm.

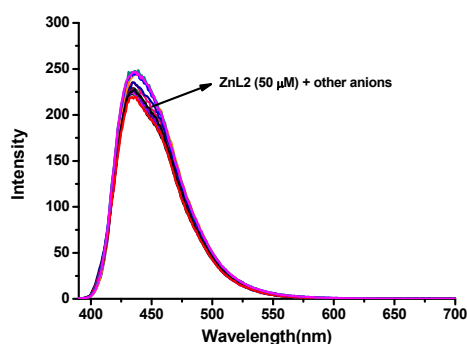


Fig. S11. Fluorescent titration of complex **ZnL2** (50 μM) upon the addition of other anions (PO_4^{3-} , HPO_4^{2-} , H_2PO_4^- , F^- , Cl^- , Br^- , I^- , ClO_4^- , AcO^- , CO_3^{2-} , HCO_3^- , SO_4^{2-} , HSO_4^- , $\text{S}_2\text{O}_7^{2-}$, $\text{S}_2\text{O}_3^{2-}$, SCN^- , NO_3^- , N_3^- , NO_2^- , 500 μM of each) in pH = 7.2, 10 mM HEPES buffer solution at 25°C, λ_{ex} = 380 nm, d_{ex} = d_{em} = 2.5 nm.

Table S1 Summary of the apparent association constants (K_a) of receptors **ZnL1** and **ZnL2** to some anion species.

Anions	K_a (M^{-1}) between receptor and anions		
	ZnL1 ^a	ZnL2 ^b (when 5 μM was used)	ZnL2 ^b (when 50 μM was used)
PPi	Not reported	5.39×10^5	7.68×10^5
NaH_2PO_4	2.9×10^5	- ^c	- ^c
ATP	4.0×10^5	8.65×10^4	6.23×10^4
ADP	1.6×10^5	- ^c	- ^c
AMP	9.1×10^3	1.37×10^4	- ^c
Citrate	Not reported	2.51×10^5	6.87×10^4

^a: Literature values (A. Ojida, Y. Mito-oka, K. Sada, I. Hamachi, *J. Am. Chem. Soc.*, 2004, **126**, 2454-2463, see page 2456). ^b: Experimental values in this work, see above figures. ^c: K_a was not determined due to too small changes of fluorescence. Note: Much higher ion strength conditions (50 mM HEPES, 50 mM NaCl, pH 7.2) were used in the literature for the K_a measurement between **ZnL1** and ATP, ADP and AMP. Take this factor into consideration, from the K_a values of ATP between **ZnL1** and **ZnL2**, introducing $-\text{CH}_2\text{OH}$ groups to **ZnL1** may decrease its binding affinities to phosphate anions.

5. The fluorescence colour changes of ZnL2 upon addition of different anions

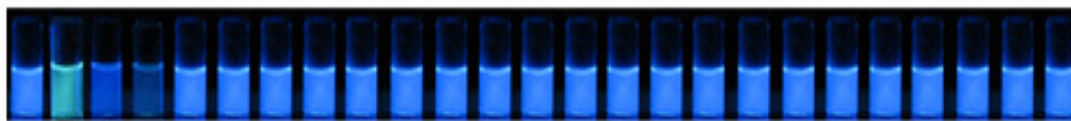


Fig. S12. Fluorescence colour (under 365 nm light) changes of **ZnL2** (50 μM) in 10 mM aqueous HEPES buffer solution (pH = 7.2) with 500 μM of different anions (from left to right: none, PPI, ATP, Citrate, ADP, AMP, PO_4^{3-} , HPO_4^{2-} , H_2PO_4^- , F^- , Cl^- , Br^- , I^- , ClO_4^- , AcO^- , CO_3^{2-} , HCO_3^- , SO_4^{2-} , HSO_4^- , $\text{S}_2\text{O}_7^{2-}$, $\text{S}_2\text{O}_3^{2-}$, SCN^- , NO_3^- , N_3^- , NO_2^-).

6. The effect of concentration of ZnL2-PPI on anthracene-excimer formation

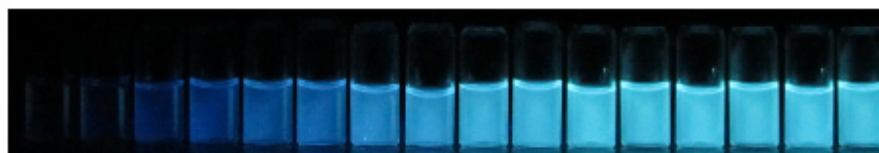
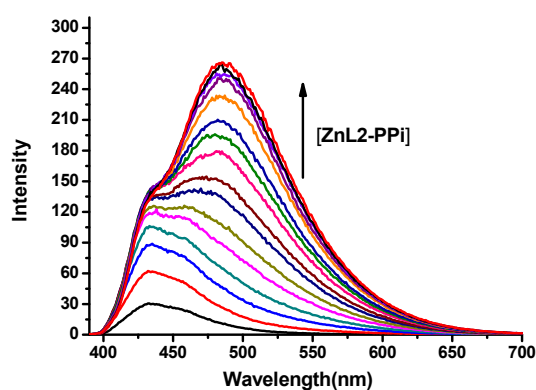


Fig. S13. Top: Fluorescent spectra of **ZnL2-PPI** (5, 10, 15, 20, 25, 30, 35, 40, 45, 50, 55, 60, 65, 70, 75 and 80 μM) in 10 mM HEPES buffer solution (pH = 7.2) at 25°C with $\lambda_{\text{ex}} = 380 \text{ nm}$, $d_{\text{ex}} = 5 \text{ nm}$, $d_{\text{em}} = 2.5 \text{ nm}$. Down: Emission color changes of **ZnL2-PPI** under UV light of 365 nm. The concentration of **ZnL2-PPI** from left to right: 5, 10, 15, 20, 25, 30, 35, 40, 45, 50, 55, 60, 65, 70, 75 and 80 μM , respectively.

7. The effect of buffer concentration and salts on PPI induced anthracene-excimer formation

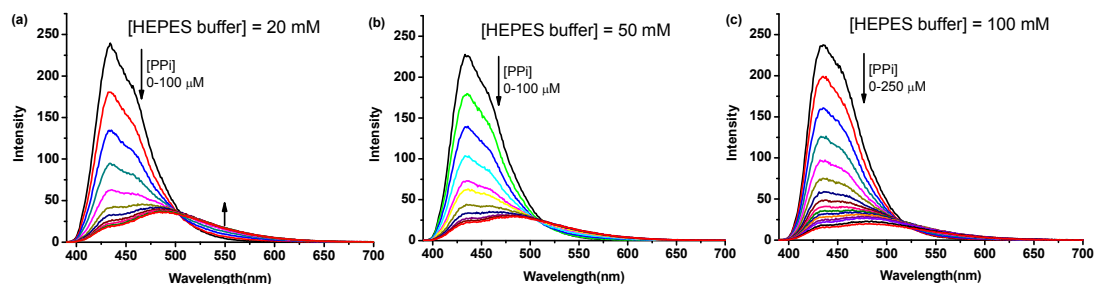


Fig. S14. The effect of buffer concentration on PPI induced anthracene-excimer formation. HEPES

buffer concentration (a) 20 mM; (b) 50 mM; (c) 100 mM. All experiments were measured at 25°C and $[\text{ZnL2}] = 50 \mu\text{M}$. These experiments indicate that the excimer formation is more difficult at higher buffer concentrations.

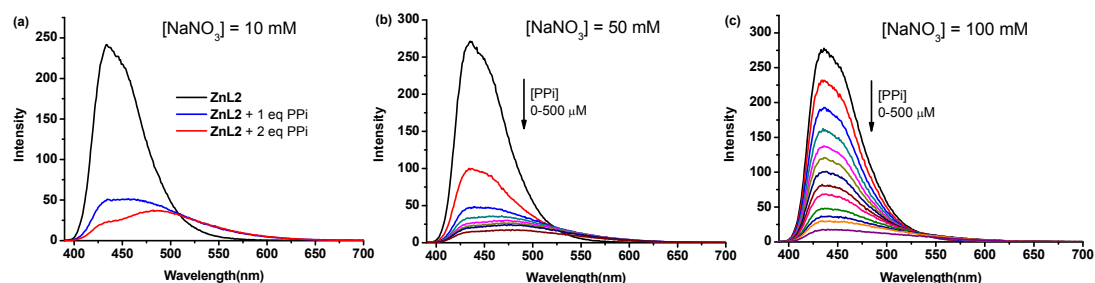


Fig. S15. The effect of presence of salts on PPI induced anthracene-excimer formation. NaNO₃ concentration (a) 10 mM; (b) 50 mM; (c) 100 mM. All experiments were measured in 10 mM HEPES buffer (pH 7.2) at 25°C and $[\text{ZnL2}] = 50 \mu\text{M}$. These experiments indicate that the excimer formation is tending to be hindered at higher salts concentrations.

8. The effect of temperature (T) on PPI induced anthracene-excimer formation

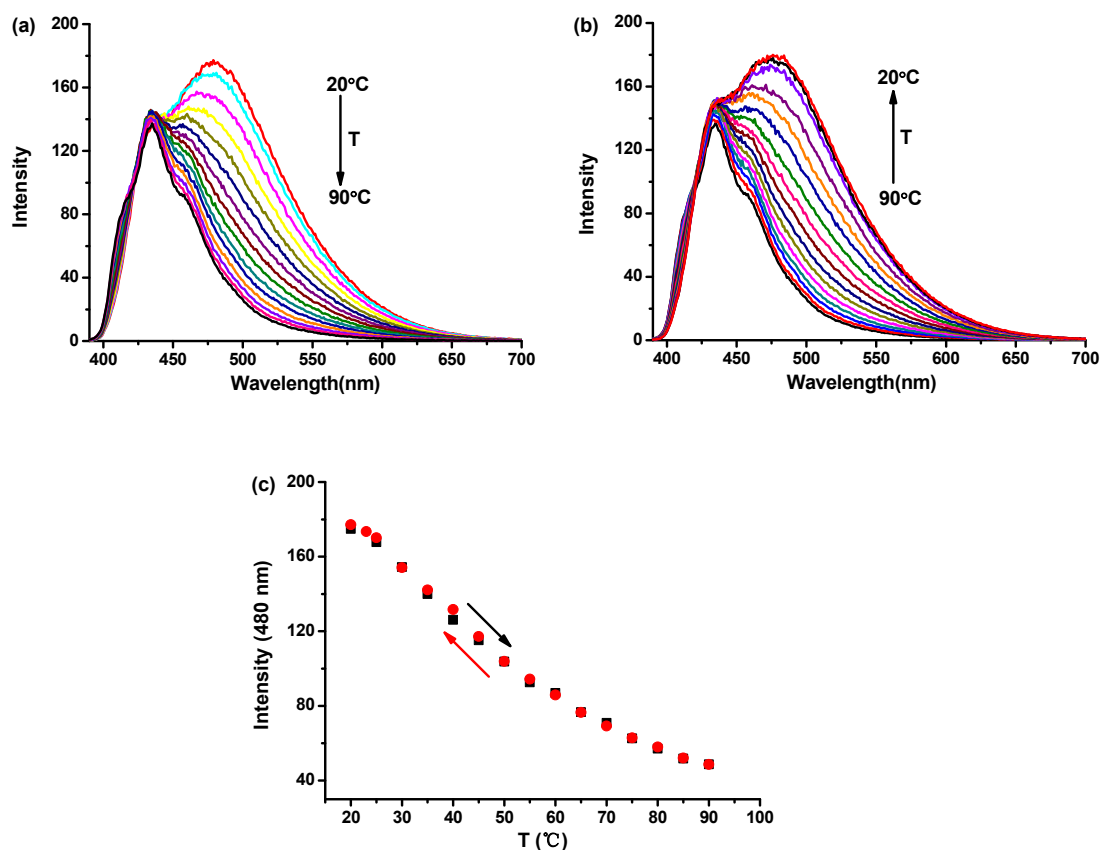


Fig. S16. (a) The fluorescence spectra changes of **ZnL2**-PPI (50 μM) as temperature increased from 20°C to 90°C. (b) The fluorescence spectra changes of **ZnL2**-PPI (50 μM) as temperature decreased from 90°C to 20°C. (c) A plot of fluorescence intensity changes of **ZnL2**-PPI (50 μM) at 480 nm as a function of temperature increase (■) or decrease (●). All spectra were measured in

10 mM HEPES buffer solution (pH = 7.2) with $\lambda_{\text{ex}} = 380 \text{ nm}$, $d_{\text{ex}} = 5 \text{ nm}$, $d_{\text{em}} = 2.5 \text{ nm}$.

9. Job's plot examined between ZnL2 and PPI, ATP and citrate

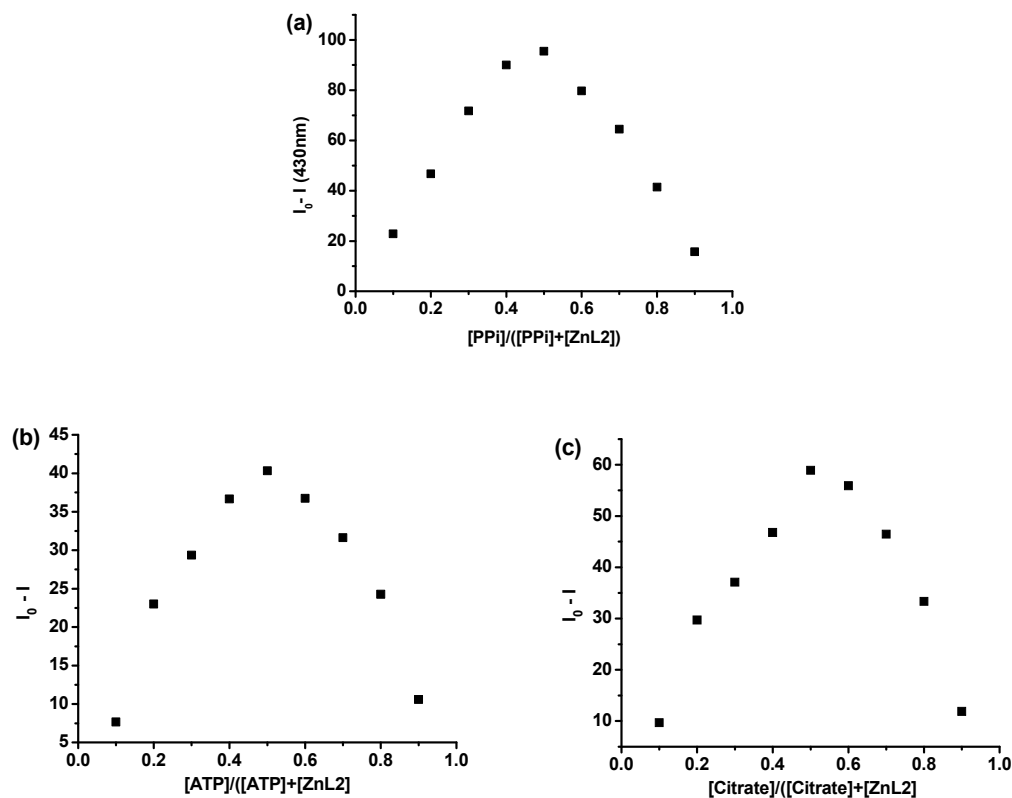


Fig. S17. Job's plot examined between **ZnL2** and PPI (a), ATP (b) and citrate (c) in 10 mM HEPES buffer (pH = 7.2) solution at 25°C. All experiments were explored at $[\text{PPI}, \text{ATP or citrate}] + [\text{ZnL2}] = 50 \mu\text{M}$ and with $\lambda_{\text{ex}} = 380 \text{ nm}$, $d_{\text{ex}} = 2.5 \text{ nm}$, $d_{\text{em}} = 2.5 \text{ nm}$.

10. The ^{31}P NMR and Mass studies

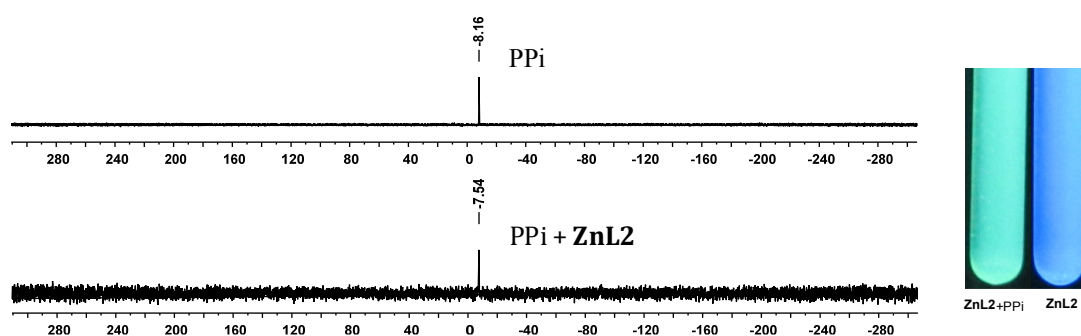
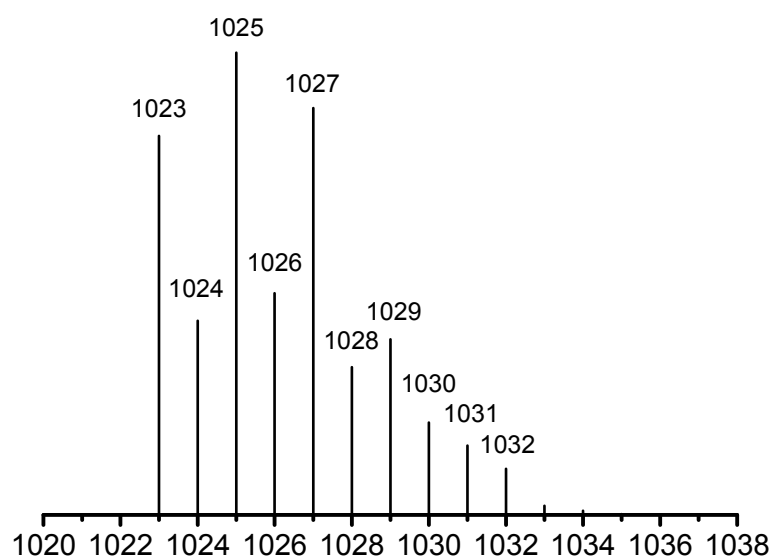
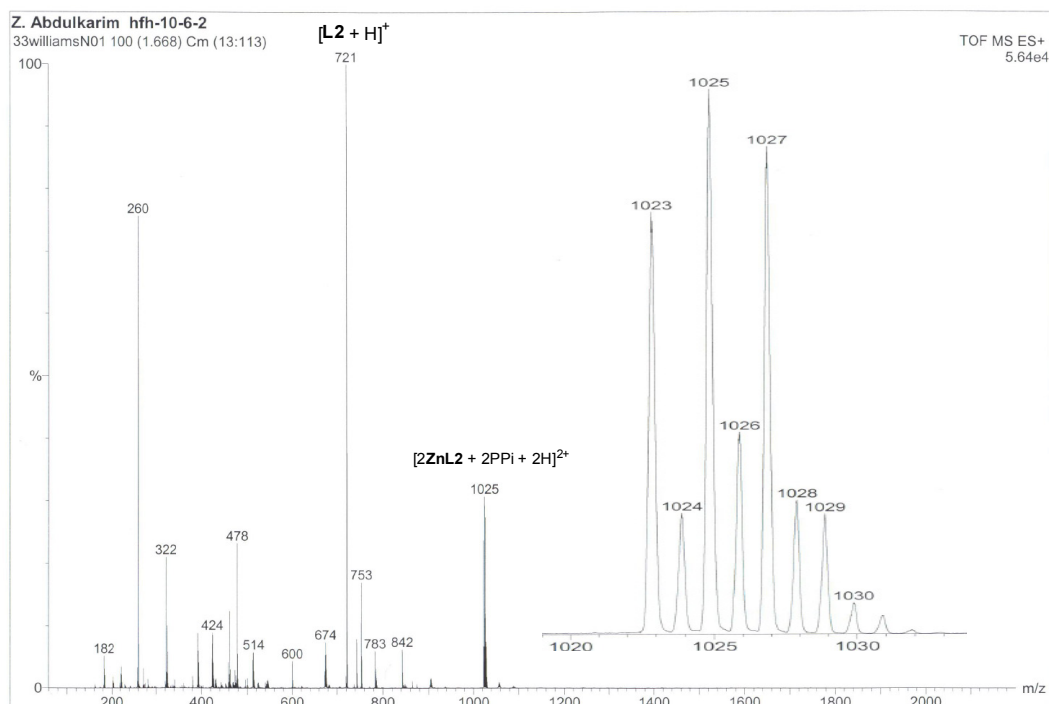


Fig. S18. Left: ^{31}P NMR spectra of PPI, and a mixture of PPI and **ZnL2** (1 mM of each) in D_2O . Right: The fluorescence color of **ZnL2** (1mM) under 365 nm in the presence and absence of PPI in the NMR tube.



Isotopic Distributions Calculated

Fig. S19. Top: Mass spectrum of a mixture of **ZnL2** and PPI (50 μ M each). The peak at $m/z = 1023$ corresponds to $[C_{88}H_{90}N_{12}O_{22}P_4Zn_4]^{2+}$ ($= [2ZnL2 + 2PPI + 2H]^{2+}$, which Mass was calculated as 2046). Bottom: Isotopic distribution calculated for $C_{44}H_{45}N_6O_{11}P_2Zn_2$ using a program in www.chemcalc.org.

Elemental Composition Report

Single Mass Analysis

Tolerance = 5.0 PPM / DBE: min = -1.5, max = 50.0

Isotope cluster parameters: Separation = 1.0 Abundance = 1.0%

Monoisotopic Mass, Odd and Even Electron Ions

3 formula(e) evaluated with 1 results within limits (up to 50 closest results for each mass)

Minimum:		-1.5				
Maximum:		200.0	5.0	50.0		
Mass	Calc. Mass	mDa	PPM	DBE	Score	Formula
1023.1177	1023.1204	-2.7	-2.7	26.5	1	C ₄₄ H ₄₅ N ₆ O ₁₁ P ₂ Zn ₂

Z. Abdulkarim hf-10-6-2

37williamsN05 106 (1.767) AM (Cen,4, 80.00, Ar,5000.0,1053.60,1.00); Cm (3:238)

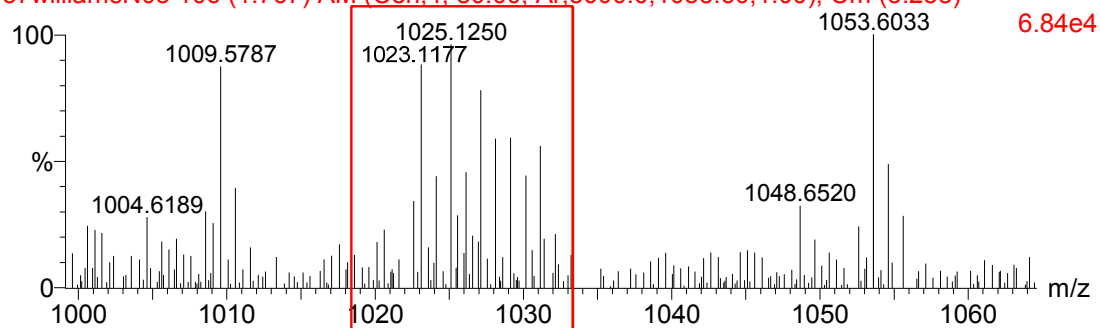


Fig. S20. High Resolution Mass spectrum of a mixture of **ZnL2** and PPI (50 μ M each). The peak at $m/z = 1023.1177$ corresponds to formula C₄₄H₄₅N₆O₁₁P₂Zn₂, which was calculated as 1023.1204.